*Geophys. J. Int.* (2002) **150,** 58–64

# The amplitude of the Love–Rayleigh discrepancy created by small-scale heterogeneities

Valérie Maupin

*Department of Geology, University of Oslo,* POB 1047 *Blindern,* 0316 *Oslo, Norway. E-mail: valerie.maupin@geologi.uio.no*

Accepted 2002 January 14. Received 2001 December 21; in original form 2001 September 7

## SUMMARY

At global as well as at regional scale, the lithosphere appears faster to Love waves than to Rayleigh waves. This Love–Rayleigh discrepancy can be modelled by introducing transverse isotropy in the upper mantle. In some regions however, it is so large that the question arises as to whether part of it could be an artefact related to the presence of heterogeneities in the lithosphere. Using a multiple-scattering scheme to model surface waves in 3-D structures, we analyse the influence of small-scale heterogeneities in the lithosphere on the Love–Rayleigh discrepancy in the period range 25 to 60 s. Small-scale heterogeneities tend to lower the apparent phase velocity of the surface waves, and have a larger effect on the Love waves than on the Rayleigh waves. This is not due to mode-coupling, which plays a negligible role here, but to the interference of the primary field with the one backscattered twice. For models with *S*-wave velocity variations of rms 2.5 per cent, and spatial correlations at distances of 20 to 100 km, we find that the Love waves are on average and at most 0.1 per cent slower than the Rayleigh waves. This apparent Love–Rayleigh discrepancy varies linearly with the variance of *S*-wave velocity variation in the structure. We conclude that small-scale heterogeneities do not contribute significantly to the large Love–Rayleigh discrepancies of 4 to 9 per cent observed in some regions, since they produce an apparent discrepancy which is negligible in comparison, and which even has the opposite sign.

**Key words:** anisotropy, inhomogeneous media, Love waves, Rayleigh waves, surface waves, wave propagation.

## 1 INTRODUCTION

Modern global seismic models of the Earth include anisotropy at different depths. The best resolved anisotropic parameter in the lithosphere is $\xi$, which expresses the difference between the velocity of horizontally propagating *SH* and *SV* waves. Globally, *SH* waves propagate faster than *SV* waves in the upper mantle. The velocity difference is of about 4 per cent in the Preliminary reference Earth model (PREM) of Dziewonski & Anderson (1981) and 3 per cent in the AK135 model of Kennett *et al.* (1995). Much of the evidence for this anisotropy comes from measurements of Love and Rayleigh wave phase velocities and the so-called Love–Rayleigh discrepancy, expressing that Love waves usually have a phase velocity larger than predicted by isotropic models that fit the phase velocity of the Rayleigh waves.

Locally, and especially in continental regions, the Love–Rayleigh discrepancy may reach values much larger than those found in global models. For example, analysing Love and Rayleigh waveforms, Debayle & Kennett (2000) infer that *SH* waves have velocities up to 9 per cent larger than *SV* waves in Australia. This velocity difference can hardly be explained by a pyrolitic mantle model where crystals would be perfectly oriented. An horizontal flow in the mantle creates a Love–Rayleigh discrepancy which varies with azimuth and which is mostly positive (i.e. *SH* waves faster than *SV* waves, as in global models), whereas a vertical flow produces a negative discrepancy without azimuthal variations (Maupin 1985). In regions of large positive discrepancy, one would thus expect to observe important azimuthal variations of the phase velocities. In Debayle & Kennett (2000), the region of large difference between *SH* and *SV* wave velocities does not correspond to the region with largest azimuthal velocity variation. In other continental regions, as in Iberia (Maupin & Cara 1992), Germany (Friederich & Huang 1996) or South Africa (Freybourger *et al.* 2001), important positive Love–Rayleigh discrepancies do not seem to be associated with strong azimuthal variations of the Rayleigh wave phase velocities. The surface wave velocity pattern in these regions is also difficult to reconcile with a geodynamic model compatible in particular with *SKS*-splitting.

Although intrinsic anisotropy is undoubtedly responsible for part of the Love–Rayleigh discrepancy, the question arises as to whether part of it could be an artefact created by propagation in laterally heterogeneous structures, as suggested by Levshin & Ratnikova (1984). In this paper, we analyse the effect of small-scale isotropic heterogeneities in the lithosphere on the phase velocities of Love and

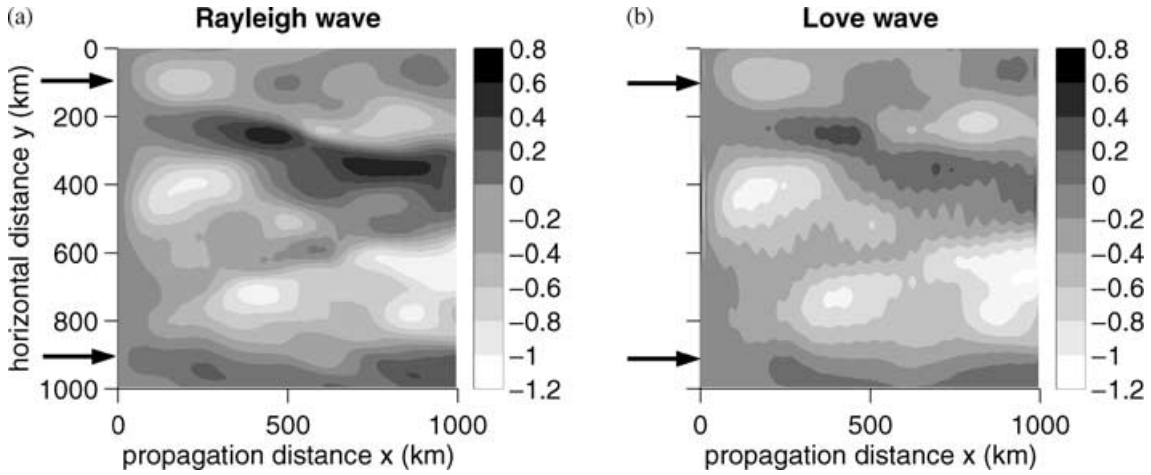


**Figure 1.** Maps of the phase anomalies of the (a) Rayleigh wave and (b) Love wave fundamental modes at 25 s period in the model shown in Fig. 2. The phase anomaly is expressed in radians. The arrows indicate the direction of the incident surface wave.

Rayleigh waves in the period range 25 to 60 s, with emphasis on the Love–Rayleigh discrepancy they can produce. By isotropic we mean that the material is isotropic, not necessarily the shape of the heterogeneities.

Heterogeneities change the apparent velocity of elastic waves in a complex way. In structures with large-scale heterogeneities, waves favour paths through fast regions and therefore appear on average to travel faster than the mean velocity of the structure would suggest (Wielandt 1987). On the other hand, small-scale heterogeneities produce multiple-scattering which tends to decrease the waves apparent velocity (Shapiro *et al.* 1996b; Herman 2001). For surface waves, heterogeneities may in addition produce mode-coupling, which may in turn modify the apparent velocity of the total wavefield. The different mechanisms may affect differently the Love and the Rayleigh waves, producing an apparent Love–Rayleigh discrepancy. The effect of small-scale heterogeneities on surface wave propagation has been studied in 2-D structures by Kennett & Nolet (1990) and Park & Odom (1999) in particular. Kennett & Nolet (1990) show that upper mantle heterogeneities on scales of 300 to 400 km and with *S*-wave deviations of $\pm 2$ per cent do not affect Rayleigh waves at periods larger than 20 s. Park & Odom (1999) develop a formalism to calculate the scattering of multimode wavefields by corrugated interfaces. They present an application in a shallow-water environment with emphasis on the attenuation of high-frequency guided waves by irregularities of the water bottom. In the present paper, we use a multiple-scattering scheme developed by Maupin (2001), which has the advantage over previous studies of being able to take into account the 3-D nature of the scattering. After a short description of the method and of the characteristics of the heterogeneous models we have used, we analyse the amplitude of the Love–Rayleigh discrepancy in models of the lithosphere with small heterogeneities at different scales, and in models of corrugated Moho.

## 2 SHORT DESCRIPTION OF THE METHOD

The wavefield is calculated with a multiple-scattering scheme for modelling surface wave propagation in 3-D structures (Maupin 2001). A monochromatic plane surface wave is incident on a 3-D heterogeneous structure, which is here a realization of a stochastic model with predefined characteristics. The structure is separated into a laterally homogeneous reference structure and superimposed lateral heterogeneities. The lateral heterogeneities, which act as secondary sources, scatter energy away from the dominant propagation direction and produce mode coupling. The method calculates the total wavefield in the 3-D structure, expressed as a sum of modes of the reference structure. No approximation is made concerning the azimuthal variation of the scattering, and in particular no assumption needs to be made on the strength of the backscattered field. The method is based on a Neumann series, which means that multiple-scattering is included in an iterative way. The first iteration gives the Born approximation, and each new iteration adds one order of scattering to the total wavefield.

As an example, Fig. 1(a) shows the phase of the vertical component of a Rayleigh wave fundamental mode at 25 s period propagating through the structure shown in Fig. 2. Fig. 1(b) shows the same for the transversal component of the Love wave fundamental mode. In both cases, the phase is measured at the free surface and we show the difference with respect to the phase in the homogeneous reference structure, which is here the PREM model (Dziewonski & Anderson 1981) with a 35 km thick continental crust. The monochromatic plane wave, which is either a pure Rayleigh wave fundamental mode or a pure Love wave fundamental mode, is incident onto the heterogeneous structure from the left, as shown by the two arrows on Figs 1(a and b). Although the wavefield loses its simple plane structure in the 3-D model, it keeps a dominant propagation direction similar to the initial one. We denote therefore the $x$-direction, or direction of initial propagation direction, simply for direction of propagation in the rest of the text. Similarly, the perpendicular horizontal direction, denoted $y$, is simply called the wave front direction.

From the phase anomaly $\phi(x, y)$ of the total wavefield, the apparent phase slowness $\delta s(x, y)$ in the structure is simply calculated by:

$$\delta s(x, y) = \frac{-T}{2\pi}\frac{1}{x}(\phi(x, y) - \phi(x_0, y)) \quad (1)$$

where $x$ is the distance in the initial propagation direction, $y$ is the horizontal distance along the incident wave front, and $T$ is the period of the wave. $x_0$ is a reference distance which we would normally set at $x = 0$. Due to boundary effects in the numerical code, it is however more appropriate to use a reference distance slightly inside the heterogeneous structure. We use $x_0 = 50$ km in the examples

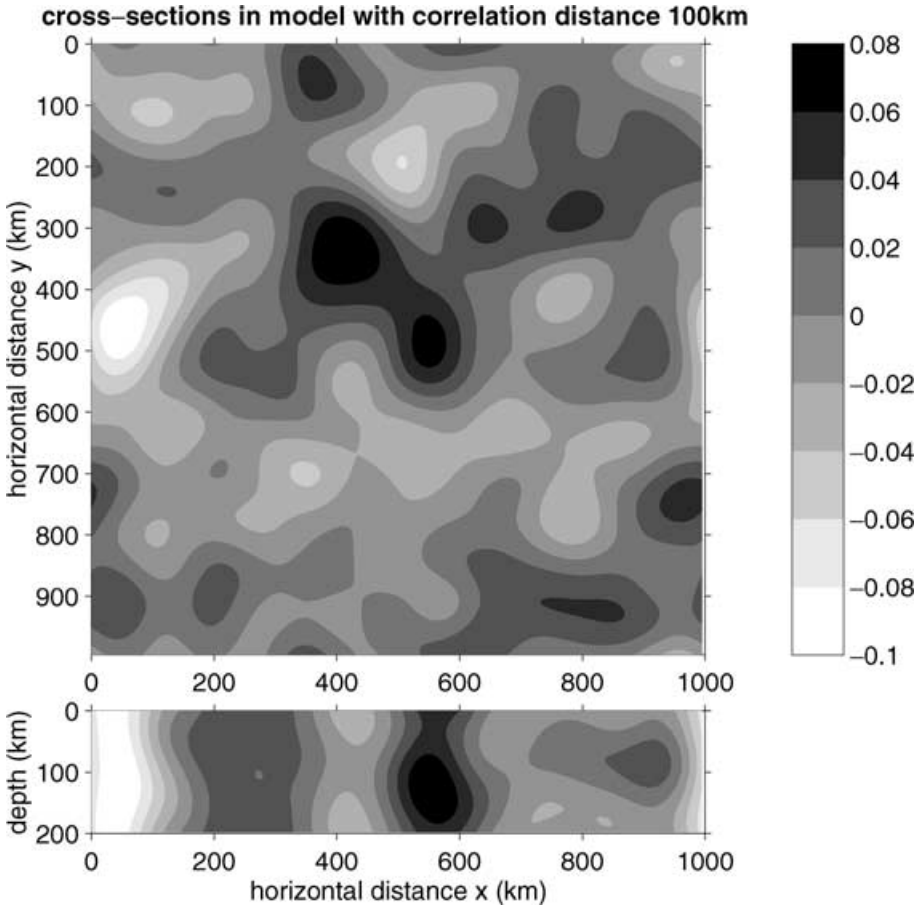


**Figure 2.** Relative variations in *S*-wave velocity in the 3-D model used to calculate the wavefields shown in Figs 1, 3 and 4. The top panel shows an horizontal cross-section at 100 km depth and the bottom panel shows a vertical cross-section at horizontal distance 500 km. The velocity variations have an rms of 2.5 per cent and a gaussian autocorrelation function with a correlation distance of 100 km.

shown in later sections. A minus sign is included to take into account the phase Fourier convention in Maupin (2001). When there are several modes involved, we use the phase of the total wavefield.

In addition, we calculate a mean phase slowness as a function of propagation distance by taking the mean over the whole wave front:

$$\delta\bar{s}(x) = 1/A \int_0^A \delta s(x, y)\, dy \tag{2}$$

where $A$ is the dimension of the model in the $y$-direction.

The results are discussed in terms of apparent phase velocity, the inverse of the apparent slowness. We calculate the phase velocity anomalies of Love and Rayleigh waves in different models and identify the possible difference in anomaly with the apparent Love–Rayleigh discrepancy. A more correct procedure would be to invert the phase velocity anomalies to give the *SH*- and *SV*-wave velocity depth profiles and to then compare the two.This would require calculating the apparent phase velocities at a much larger number of periods, instead of at two periods only as we are doing now. Our simplified procedure is valid only if the partial derivatives of the Love and Rayleigh wave phase velocities are sufficiently similar. We tested that point by inverting a constant Rayleigh wave phase velocity anomaly over a period range of 15 to 100 s into an *S*-wave velocity perturbation with depth, and then calculating the Love wave phase velocity anomaly produced by this model perturbation. In PREM-like models and at 25 s period, this resulted in phase velocity anomalies for Love waves about 20 per cent larger than for Rayleigh waves. This difference would not affect our conclusions and we can assume that our simplified approach gives a reasonable evaluation of the Love–Rayleigh discrepancy.

## 3 CHARACTERISTICS OF THE MODELS

Fig. 2 shows two cross-sections of the 3-D model in which the wavefields shown in Fig. 1 are calculated. Lateral variations are located from 0 to 200 km depth. The *S*-wave velocity variations have an rms of 2.5 per cent and a spatial correlation following a gaussian function with a correlation length of 100 km. The model has been generated by 3-D inverse Fourier transformation of a spectrum with random phase and power spectrum proportional to $\exp(-a^2k^2/4)$, where $k$ is the amplitude of the circular wavenumber vector, and $a$ is the correlation length (100 km in the present model). The relative *P*-wave velocity and density variations follow the relative *S*-wave velocity variations, with amplitude ratios of 1 for the *P*-wave velocity and 0.4 for the density.

Two other models with smaller correlation distances have also been used. The first one has correlation lengths equal to 20 km in all directions, and the second one has correlation lengths equal to 100 km in the two horizontal directions and 20 km in the vertical direction. These correlation lengths have been chosen in order to test the influence on the Love–Rayleigh discrepancy of heterogeneities at a scale similar to the wavelength and smaller. Heterogeneities

larger than 500 km in horizontal dimensions, or larger than the wavelength, are not analysed here as they would require models with dimensions which would necessitate using another numerical technique to calculate the wavefield.

The rms variation in our models is 2.5 per cent, leading to peak-to-peak variations of about 15 per cent. Rms variation of the same magnitude but at smaller correlation lengths have been found in the upper mantle by array studies using short-period *P* waves (Charette 1991; Hestholm *et al.* 1994; Wu & Flatté 1990). Models of the *S*-wave velocity variation at these correlation distances are more sparse. Igel & Gudmundsson (1997) model *S*-wave propagation in the mantle at periods similar to ours. Their model with largest rms variation and smallest correlation length is similar to the model shown here in Fig. 2. Nolet & Moser (1993) analyse the effect of mantle heterogeneities on the *S*-wave dispersion and favour a model with upper mantle variations with rms of 3.5 per cent at 200 km correlation length.

As changes in crustal thickness influence Love and Rayleigh wave phase velocities differently and may bias estimates of the Love–Rayleigh discrepancy (Debayle & Kennett 2000), we analyse also the effect of Moho corrugations. We use two models with depth variations of the Moho having an rms of 1 km, like in Hestholm *et al.* (1994), and with spatial correlations following gaussian functions with correlation distances of 20 and 100 km.

The horizontal dimensions of the models are 1000 km, with a sampling interval of 5 km. Numerical considerations are of course a limiting factor when choosing the dimensions of the model. It has, however, to be large enough to be representative of a random structure, and to ensure that wave phenomena such as wave front healing converge sufficiently. Significant Love–Rayleigh discrepancies have been observed by interstation phase measurements over regions which are not more than a few hundred kilometres wide (Wielandt *et al.* 1987; Friederich & Huang 1996; Maupin & Cara 1992; Freybourger *et al.* 2001). Measuring apparent phase velocity over a distance of 1000 km should therefore be sufficient to test if this observed discrepancy is biased by small-scale heterogeneities. The sampling interval of 5 km has been chosen to ensure a good representation of the forward as well as backscattered fields.

## 4 RESULTS IN MODEL WITH 100 KM CORRELATION DISTANCE

Fig. 1 shows the phases of the Rayleigh and Love waves at 25 s period in the model shown in Fig. 2, with small-scale heterogeneities having correlation distances of 100 km in all directions. We notice that the pattern of phase variation is very similar for the two waves and follows obviously the zones of high and low velocities in the model. The amplitude of the phase variation is significant, with a total variation of about $\pi/2$. The pattern is more smooth for the Rayleigh wave than for the Love wave, for which we can see an interference pattern related to the presence of stronger reflected waves. Let us also note that large amplitude variations occur across the structure. The effect on the amplitudes is larger than on the phases. This is not surprising as phases, or traveltimes, are usually a more stable element in the wavefield than the amplitudes. In this model, the amplitude of the Rayleigh wave varies by a factor of 6 across the structure, and the amplitude of the Love wave by a factor of 3. This proves that the strength of heterogeneity we have chosen is not small and is able to produce significant effects on the wavefield.

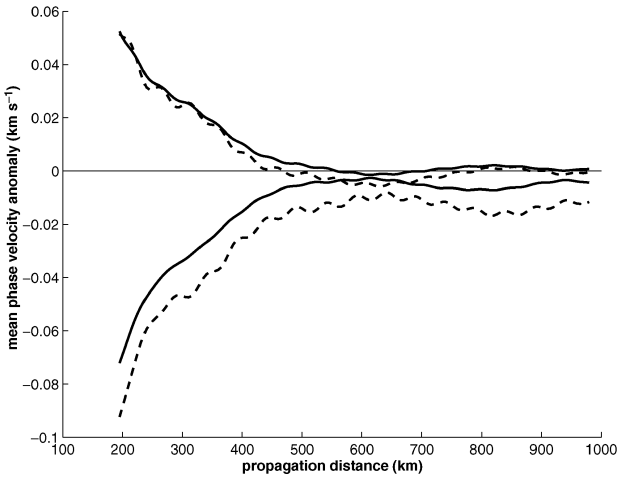


**Figure 3.** Mean phase velocity anomaly as a function of propagation distance in the model shown in Fig. 2 (2 lowest curves) and in a model with opposite velocity variations (2 upper curves). The velocity anomalies for Rayleigh waves are shown as solid lines and for Love waves as dashed lines.

### 4.1 Amplitude of the Love–Rayleigh discrepancy

The two lowest curves of Fig. 3 show the mean phase velocity anomalies for the Rayleigh and Love waves, derived from the phases shown in Fig. 1, and plotted as a function of propagation distance into the 3-D structure. Although they start at a propagation distance of 200 km, meaningful values are obtained only for propagation over at least a few correlation lengths, that is at the largest propagation distances in the present model.

The two upper curves show the apparent velocities in a model identical to the one presented in Fig. 2, but with opposite velocity variations. This enables us to separate in the phase velocity anomalies the bias related to the particular model we are using, which changes sign when changing model, from the part which is more intrinsically related to the fact that the model has small-scale heterogeneities.

The two Rayleigh wave apparent velocities vary in a symmetric way, but their mean is slightly below zero. This is similar for Love waves, but with a mean at a low velocity. Modelling other realizations of the same random structure gave similar results. Heterogeneities tend to reduce the apparent velocities of the Rayleigh waves less than of the Love waves, which are on the average slower than Rayleigh waves by 0.005 km $s^{-1}$, or about 0.1 per cent.

In addition to calculating the mean phase velocity variation along the wave front, we analyse the apparent velocity at different points along the wave front by plotting $\delta c(x, y)$ as a function of $x$ for different $y$ values. This corresponds more closely to an observational situation where the phase at two different isolated stations are used to calculate the interstation phase velocity. The Love–Rayleigh discrepancy, or difference between the phase velocity anomaly of the Love wave and phase velocity anomaly of the Rayleigh wave, is shown in Fig. 4 for propagation distances larger than 200 km. Although there is of course some scatter in the Love–Rayleigh discrepancy measured at different $y$-locations, most values are below 0 from 700 to 1000 km propagation distance, and the rms of the discrepancy is smaller than the mean discrepancy itself.

### 4.2 Effect of mode-coupling

The results shown here are those calculated with one mode only. Mode coupling, either Love–Love, Rayleigh–Rayleigh or

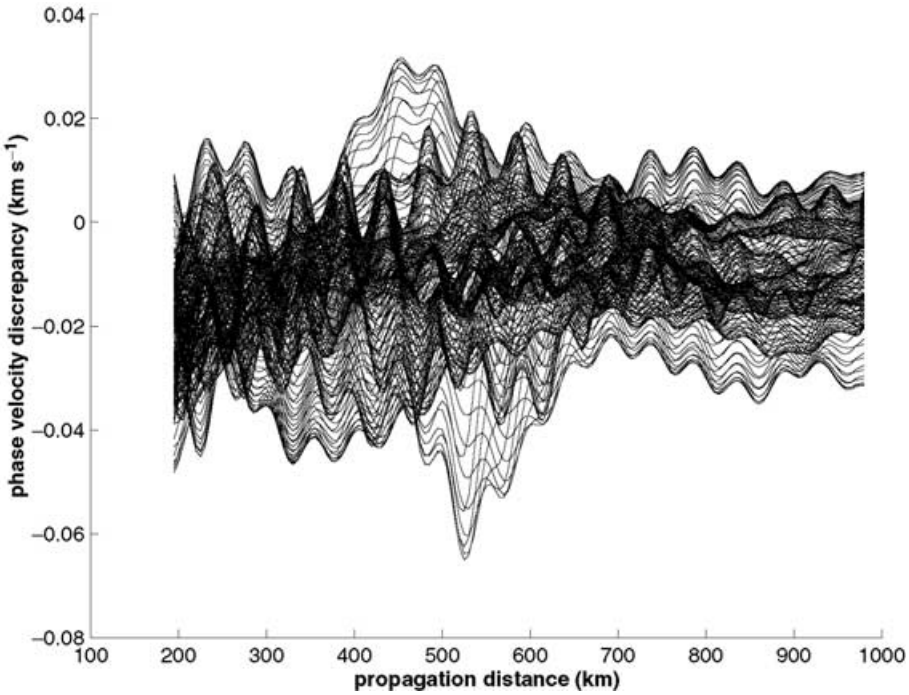


**Figure 4.** Love–Rayleigh discrepancy as a function of propagation distance in the model shown in Fig. 2, measured along lines located every 5 km and perpendicular to the initial wave front.

Love–Rayleigh coupling, proved to be negligible in all the stochastic models we have tried. As an example, taking into account the coupling of the fundamental mode of the Love wave with its first overtone decreases the mean apparent phase velocity by only 0.0005 km $s^{-1}$. This is because the amplitude of the first overtone reaches only 2 per cent of the amplitude of the fundamental mode, and is not able to modify significantly the phase of the total field. For Rayleigh waves, the relative amplitude of the first overtone generated by coupling to the fundamental mode reaches only 1 per cent and the apparent phase velocity modification due to this coupling is even smaller than for Love waves. Similarly, Love–Rayleigh coupling modifies the apparent phase velocities by at most $5 \times 10^{-5}$ km $s^{-1}$. Altogether, mode-coupling does not contribute to the Love–Rayleigh discrepancy we measure in small-scale heterogeneous structures. Neglecting it modifies the Love–Rayleigh discrepancy by at most 10 per cent.

### 4.3 Effect of multiple-scattering

In all the examples we show, the wavefield includes waves scattered up to three times, but the results are very similar with two orders of scattering only. On the other hand, there is no Love–Rayleigh discrepancy at only one order of scattering. The amplitude of the discrepancy varies with the variance of the lateral variations. Taking into account the scale difference, the reduction in velocity which we find for Love waves is actually similar to the one found by Shapiro *et al.* (1996a) for high-frequency *P* waves in stochastic 1-D models. At a wavelength of four times the correlation length, they find a velocity reduction of 2.5 per cent in models with 15 per cent rms variation. Assuming a quadratic variation, that would produce a velocity reduction of nearly 0.1 per cent for an rms of 2.5 per cent. A quantitative comparison with the 2-D results of Herman (2001) is more difficult as he considers only density variations.

These different results lead us to conclude that the dominant mechanism which affects the phase of surface waves in structures with small-scale heterogeneities is, as for body waves, the interference of the primary field with the one which is backscattered twice. This yields a decrease of the apparent velocity which is proportional to the square of the strength of the backscattered field. Inspection of the azimuthal pattern of scattered surface waves shows that the Love waves have a strong backscattered field relative to Rayleigh waves (Snieder 1986; Maupin 2001). This is also apparent in Fig.1, where the interference of the primary field with a backscattered field is much more apparent for the Love wave than for the Rayleigh wave. The velocity decrease is therefore usually stronger for the Love wave than for the Rayleigh wave, leading to a negative Love–Rayleigh discrepancy.

### 4.4 Results at longer period

At 60 s period, the mean apparent discrepancy is smaller than at 25 s by a factor of 2. In addition, there is more scatter than in Fig. 4 in the discrepancies measured at different *y* locations.

## 5 RESULTS IN MODELS WITH SMALLER CORRELATION DISTANCES

In Figs 5 and 6, we show the mean phase velocity discrepancies measured in two models with smaller correlation distances.

The model used in Fig. 5 has correlation distances equal to 100 km in the two horizontal directions and 20 km in the vertical one. Due to smaller correlation lengths in the vertical direction, the mode-coupling is even smaller here than in the previous section. The mean Love–Rayleigh discrepancy, equal to $-0.003$ km $s^{-1}$, is only slightly smaller than in the previous case.

For a model with correlation distances of 20 km in all directions, convergence to a stable Love–Rayleigh discrepancy occurs at

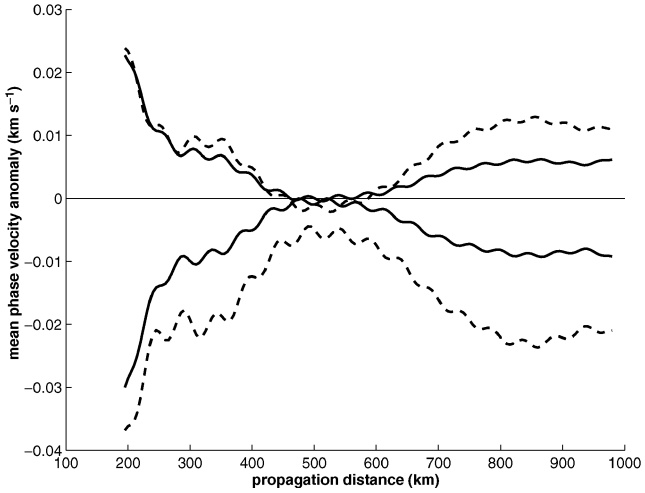


**Figure 5.** The same as Fig. 3 for a model with 100 km correlation distances in the horizontal directions and 20 km in the vertical direction.

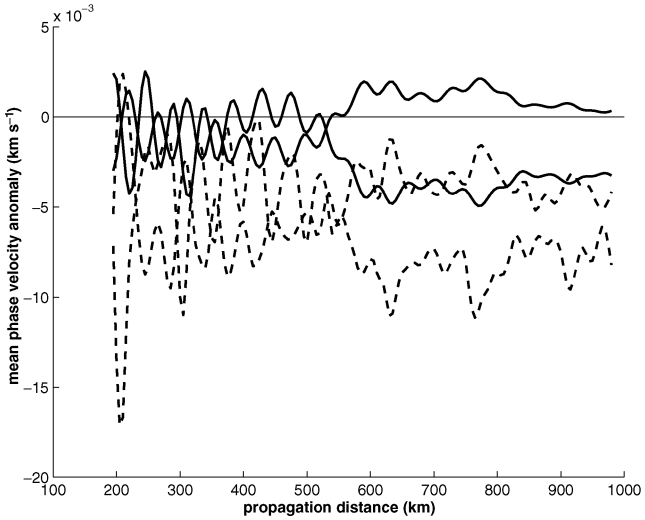


**Figure 6.** The same as Fig. 3 for a model with 20 km correlation distances in all directions.

smaller propagation distances, as can be seen in Fig. 6. In this case, the Love–Rayleigh discrepancy is the dominant feature of the figure, and variations related to changing sign of the heterogeneities are smaller. As in the other models, the apparent phase velocity of the Love waves decreases more than the apparent phase velocity of the Rayleigh waves, leading to a negative Love–Rayleigh discrepancy equal to $-0.004$ km s$^{-1}$. Despite the smaller correlation lengths, there are still significant variations of $\pm 0.01$ km s$^{-1}$ in the apparent phase velocities measured at different *y*-locations. If one can allow for larger variations at these correlation lengths, the Love–Rayleigh discrepancy can increase to 0.015 km s$^{-1}$ at 25 s period, equivalent to 0.4 per cent of the phase velocity, and 0.13 km s$^{-1}$ at 60 s period.

## 6 RESULTS IN MODELS WITH CORRUGATED MOHO

Fig. 7 shows the mean apparent phase velocity of Rayleigh and Love waves propagating in a model with a corrugated Moho discontinuity. The rms of the Moho depth variation is 1 km, as in the models of Hestholm *et al.* (1994), and the correlation distance is 20 km. The

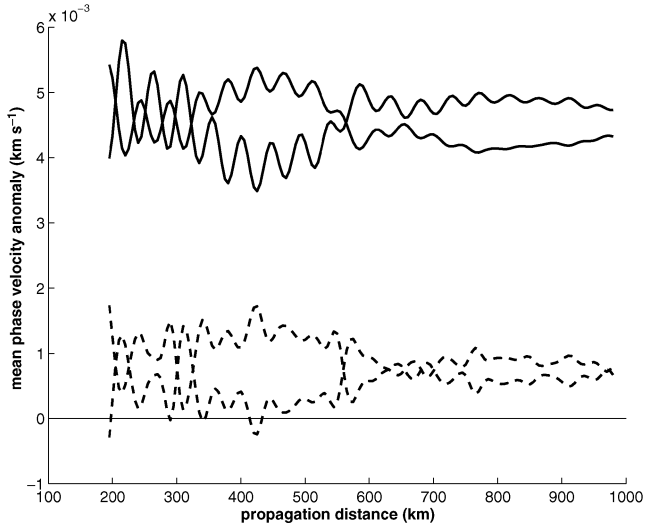


**Figure 7.** The same as Fig. 3 for a model with corrugated Moho. The rms of the Moho variation is 1 km and the correlation distance is 20 km.

main difference with the results in 3-D models is that the phase velocity anomalies are dominantly positive. The Love waves are still slower than the Rayleigh waves, but the Love–Rayleigh discrepancy is of only $-3 \times 10^{-3}$ km s$^{-1}$, that is a factor of 10 smaller than for the 3-D heterogeneities of the previous section. Similar values of Love–Rayleigh discrepancies are found in models with correlation distances of 100 km.

## 7 CONCLUSION

Lithospheric small-scale heterogeneities do not perturb strongly or very differently the phase velocities of the Love and Rayleigh waves in the period range 25 to 60 s. They produce no significant mode-coupling. They reduce slightly the waves apparent phase velocities by a mechanism which is similar to the one acting on body waves: energy backscattered twice interferes with the primary wavefield with a delay, and thus reduces the waves apparent phase velocity. Since backscattering is usually stronger for Love waves than for Rayleigh waves, the reduction in velocity is larger for the Love waves, producing on average a negative Love–Rayleigh discrepancy.

The amplitude of the discrepancy is not strongly dependent on the correlation distances in the models, and varies linearly with the variance of the velocity variations. For rms variations of 2.5 per cent, leading to peak-to-peak variations of the order of 15 per cent, we find an average Love–Rayleigh discrepancy of about $-0.004$ km s$^{-1}$, or $-0.1$ per cent at 25 s period, and $-0.05$ per cent at 60 s period. This is negligible compared to the Love–Rayleigh discrepancies of 4 to 9 per cent which are observed, and has in addition the opposite sign. Corrugations of the Moho discontinuity with an rms of 1 km produces even smaller effects.

Our knowledge of the amplitude of the actual small-scale *S*-wave velocity variations in the lithosphere is of course very poor. However, considering the difference in amplitude between the observed and the apparent Love–Rayleigh discrepancy we measure here, the fact that they have opposite signs, and the fact that the models we have been using produce significant wave amplitude variations, increasing the variance in the models does not seem to be an option for better explaining the observed discrepancy.

Very large Love–Rayleigh discrepancies, which are difficult to explain with realistic models of lithospheric anisotropy, or which

do not fit with other seismological data like *SKS*-splitting measurements, cannot be explained by the effect of small-scale lateral heterogeneities. As this study is limited to models with heterogeneities at scales smaller than about 500 km, this of course does not preclude that larger scale heterogeneities, like continental margins, large Moho depths variations, or regional heterogeneities, may be responsible for part of the discrepancy. This kind of larger scale variation may introduce non linear phenomena, like mode-coupling or ray-bending, which are usually not accounted for in the procedures used to analyse the data, and which may affect differently the Love and the Rayleigh waves. Wang & Dahlen (1994) showed that in the period range 150 to 450 s, ray-bending in global models produces an apparent Love–Rayleigh discrepancy of 0.02 to 0.1 per cent. One can expect larger effects on shorter period waves, since they are more affected by larger velocity variations in the upper part of the lithosphere and are more sensitive to regional scale variations.

The interpretation of the data in terms of lithospheric anisotropy is usually limited to rather simple anisotropic structures and to the assumption that mineral orientation alone is responsible for the anisotropy. We have also to explore the possibility of other forms of anisotropy in the lithosphere, and analyse in more detail the effect on wave propagation of more complex anisotropic structures, for example with small-scale variations as proposed by Jordan & Gaherty (1995). One should also keep in mind that there is a trade-off between density and anisotropy in the models resulting from inversion of Love and Rayleigh wave phase velocities. Although inverting the Love–Rayleigh discrepancy for density variations alone leads to unrealistic models (Cara *et al.* 1983), the presence of low-density layers in the lithosphere not accounted for in the inversion would affect the amplitude of the Love–Rayleigh discrepancy.

## ACKNOWLEDGMENTS

I wish to thank E. Husebye and B.O. Ruud for providing a copy of their code for generating 2-D stochastic structures, and G. Herman and J. Trampert for their reviews of the manuscript.

## REFERENCES

Cara, M., Lévêque, J.-J. & Maupin, V., 1983. Density-versus-depth models from multimode surface waves, *Geophys. Res. Lett.,* **11,** 633–636.

Charette, E.E., 1991. Elastic wave scattering in laterally inhomogeneous media, *PhD thesis,* MIT, Cambridge, MA.

Debayle, E. & Kennett, B.L.N., 2000. Anisotropy in the Australian upper mantle from Love and Rayleigh waveform inversion, *Earth planet. Sci. Lett.,* **184,** 339–351.

Dziewonski, A.M. & Anderson, D.L., 1981. Preliminary reference Earth model, *Phys. Earth planet. Inter.,* **184,** 297–356.

Freybourger, M., Gaherty, J.B., Jordan, T.H. & the Kaapvaal Seismic Group, 2001. Structure of the Kaapvaal craton from surface waves, *Geophys. Res. Lett.,* **28,** 2489–2492.

Friederich, W. & Huang, Z.-X., 1996. Evidence for uppermantle anisotropy beneath southern Germany from Love and Rayleigh wave dispersion, *Geophys. Res. Lett.,* **23,** 1135–1138.

Herman, G.C., 2001. Transmission of elastic waves through solids containing small-scale heterogeneities, *Geophys. J. Int.,* **145,** 436–446.

Hestholm, S.O., Husebye, E.S. & Ruud, B.O., 1994. Seismic wave propagation in complex crust-upper mantle media using 2-D finite-difference synthetics, *Geophys. J. Int.,* **118,** 643–670.

Igel, H. & Gudmundsson, O., 1997. Frequency-dependent effects on travel times and waveforms of long-period S and SS waves, *Phys. Earth planet. Inter.,* **104,** 229–246.

Jordan, T.H. & Gaherty, J.B., 1995. Stochastic modeling of small-scale anisotropic structures in the continental upper mantle, in *Proc. 17th Ann. Seismic Res. Symp.,* pp. 433–451, eds Lewkowicz, J.F., McPhetre, J.M. & Reide, D.T., Phillips Labs, Hanscom Air Force base, MA.

Kennett, B.L.N. & Nolet, G., 1990. The interaction of the S wavefield with upper mantle heterogeneity, *Geophys. J. Int.,* **101,** 751–762.

Kennett, B.L.N., Engdahl, E.R. & Buland, R., 1995. Constraints on seismic velocities in the Earth from travel-times, *Geophys. J. Int.,* **122,** 108–124.

Levshin, A. & Ratnikova, L., 1984. Apparent anisotropy in inhomogeneous media, *Geophys. J. R. astr. Soc.,* **76,** 65–69.

Maupin, V., 1985. Partial derivatives of surface wave phase velocities for flat anisotropic models, *Geophys. J. R. astr. Soc.,* **83,** 379–398.

Maupin, V., 2001. A multiple-scattering scheme for modelling surface wave propagation in isotropic and anisotropic three-dimensional structures, *Geophys. J. Int.,* **146,** 332–348.

Maupin, V. & Cara, M., 1992. Love–Rayleigh wave incompatibility and possible deep upper mantle anisotropy in the Iberian peninsula, *Pure appl. Geophys.,* **138,** 429–444.

Nolet, G. & Moser, T.-J., 1993. Teleseismic delay times in a 3-D Earth and a new look at the S discrepancy, *Geophys. J. Int.,* **114,** 185–195.

Park, M. & Odom, R.I., 1999. The effect of stochastic rough interfaces on coupled-mode elastic waves, *Geophys. J. Int.,* **136,** 123–143.

Shapiro, S.A., Hubral, P. & Ursin, B., 1996. Reflectivity/transmissivity for one-dimensional inhomogeneous random elastic media: dynamic-equivalent-medium approach, *Geophys. J. Int.,* **126,** 184–196.

Shapiro, S.A., Schwarz, R. & Gold, N., 1996. The effect of random isotropic inhomogeneities on the phase velocity of seismic waves, *Geophys. J. Int.,* **127,** 783–794.

Snieder, R., 1986. 3-D linearized scattering of surface waves and a formalism for surface wave holography, *Geophys. J. R. astr. Soc.,* **84,** 581–605.

Wang, Z. & Dahlen, F.A., 1994. JWKB surface-wave seismograms on a laterally heterogeneous earth, *Geophys. J. Int.,* **119,** 381–401.

Wielandt, E., 1987. On the validity of the ray approximation for interpreting delay times, in *Seismic Tomography,* pp. 85–98, ed. Nolet, G., Reidel Publ., Dordrecht.

Wielandt, E., Sigg, A., Plesinger, A. & Horalek, J., 1987. Deep structure of the Bohemian massif from phase velocities of Rayleigh and Love waves, *Studia Geoph. et Geod.,* **31,** 121–127.

Wu, R.S. & Flatté, S.M., 1990. Transmission fluctuations across an array and heterogeneities in the crust and upper mantle, *Pure appl. Geophys.,* **132,** 175–196.